

N-Body Simulations of Gas-Free Disc Galaxies with SMBH Seed in Binary Systems

R. Chan

Coordenação de Astronomia e Astrofísica, Observatório Nacional, Rio de Janeiro, RJ, Brazil

Email: chan@on.br

How to cite this paper: Chan, R. (2019) N-Body Simulations of Gas-Free Disc Galaxies with SMBH Seed in Binary Systems. *International Journal of Astronomy and Astrophysics*, 9, 173-190.
<https://doi.org/10.4236/ijaa.2019.93013>

Received: May 1, 2019

Accepted: July 6, 2019

Published: July, 2019

Copyright © 2019 by author(s) and Scientific Research Publishing Inc. This work is licensed under the Creative Commons Attribution International License (CC BY 4.0).

<http://creativecommons.org/licenses/by/4.0/>



Open Access

Abstract

We have shown the outcome of N-body simulations of the interactions of two disc galaxies without gas with the same mass. Both disc galaxies have halos of dark matter, central bulges and initial supermassive black hole (SMBH) seeds at their centers. The purpose of this work is to study the mass and dynamical evolution of the initial SMBH seed during a Hubble cosmological time. It is a complementation of our previous paper with different initial orbit conditions and by introducing the SMBH seed in the initial galaxy. The disc of the secondary galaxy has a coplanar or polar orientation in relation to the disc of the primary galaxy and their initial orbit are eccentric and prograde. The primary and secondary galaxies have mass and size of Milky Way with an initial SMBH seed. We have found that the merger of the primary and secondary discs can result in a final normal disc or a final warped disc. After the fusion of discs, the final one is thicker and larger than the initial disc. The tidal effects are very important, modifying the evolution of the SMBH in the primary and secondary galaxy differently. The mass of the SMBH of the primary galaxy has increased by a factor ranging from 52 to 64 times the initial seed mass, depending on the experiment. However, the mass of the SMBH of the secondary galaxy has increased by a factor ranging from 6 to 33 times the initial SMBH seed mass, depending also on the experiment. Most of the accreted particles have come from the bulge and from the halo, depleting their particles. This could explain why the observations show that the SMBH with masses of approximately $10^6 M_{\odot}$ is found in many bulgeless galaxies. Only a small number of the accreted particles has come from the disc. In some cases of final merging stage of the two galaxies, the final SMBH of the secondary galaxy was ejected out of the galaxy.

Keywords

Simulation, Disc Galaxy, Supermassive Black Hole, Binary Galaxies, Merger, Warped Disc Galaxies

1. Introduction

It is well known in the literature that supermassive black holes (SMBH) exist in the majority of the galaxies, within elliptical, disc to even in dwarf galaxies [1] [2].

Several recent works in numerical simulations with SMBH with gas [3] [4] [5] show us how complex is the dynamical evolution and mass growing with gas accretion can be.

Moreover, many papers have been published about simulations of binary mergers with BH seeds including complex dissipative processes but not included in the present simulations [6]-[14].

Simulations of binary mergers with BH seeds and no dissipative effects, similar to the ones presented in this work are published by several authors [15]-[22].

On the other hand, there are only few works in the literature based on simulations of interaction of gas-free disc galaxies [23]-[29], but none has treated the problem of the existence of a SMBH at the center of the galaxies.

In a recent paper of Li *et al.* (2017), it is presented the results of the gas-free interaction of SMBHs in very eccentric galaxy orbits. Besides, there are rare works studying the evolution of such a binary galaxy in a long interval of time [28] [29] [30] in small eccentricity orbits. This work is a complementation of our previous work [29] where, there, the focus was the evolution of the discs, but here we use different initial orbit conditions and with a SMBH seed in the initial galaxy. Thus, differently, we will focus in the SMBH seed evolution in a cosmological time and covering a wider range of orbits of the galaxy binary than in the work of Li *et al.* (2017).

Thus, the main goal of the present work is to perform numerical N-body simulations to study the time evolution of the mass and dynamics of the initial SMBH seed in the two disc galaxies. We also want to know if the tidal forces affect the evolution of the SMBH.

This paper explores the scenario as follows: first, we assume a disc galaxy with the characteristics of the Milky Way (disc, bulge, halo and SMBH). Second, we let a secondary galaxy with the same characteristics orbit on prograde coplanar or polar disc (orientation in relation to the primary disc galaxy).

The paper is organized as follows: in Section 2, we describe the numerical method used in the simulations. In Section 3 we present the initial conditions. In Section 4, we describe the results of the simulations. Finally, in Section 5, we summarize the results.

2. Numerical Method

The N-body simulation code used was GADGET [31]. A modified version of this basic code was made in order to introduce the SMBH gravitational interaction with the other particle. Here we have used only the N-body integration but without gas.

The units used in all the simulations are $G = 1$, [length] = 4.500 kpc, [mass] = $5.100 \times 10^{10} M_{\odot}$, [time] = 1.993×10^7 years ($H_0 = 100$ km/s/Mpc) and [velocity] = 220.730 km/s. Hereinafter, all the physical quantities will be referred to these units. The Hubble time t_H corresponds to 490 time units. We assumed in all the simulations the tolerance parameter $\theta = 0.577$. The energy is conserved to better than 6% during the entire evolution with a time step size $\Delta t = 1.000 \times 10^{-3}$ and the softening parameter $\epsilon = 8.000 \times 10^{-4}$.

As mentioned above, we have utilized in this work a modified version of the GADGET code [31] in order to mimic the interaction of the galaxy particles with the SMBH particle. We have assumed that the collisions between the galaxy particles and the SMBH particle are inelastic. The collision is in such a way that they fuse with the SMBH particle with the total mass as a sum of the two ones.

The Schwarzschild radius of the SMBH is defined as

$$R_{bh} = \frac{2M_{bh}}{c^2}, \quad (1)$$

where M_{bh} is the SMBH mass and c is the light velocity.

We also have assumed if a galaxy particle with softening parameter ϵ and it grazes the Schwarzschild radius of the SMBH, following the Equation (2), they are merged with one single SMBH particle (see **Figure 1**). Thus, the Schwarzschild radius increases because of the additional merged galaxy mass particle with the SMBH.

Definition of the condition when there is a merge between the galaxy and the SMBH particle

$$D \leq R_{bh} + \epsilon, \quad (2)$$

where D is the distance between the centers of the SMBH and the galaxy particle, ϵ is the particle softening parameter and R_{BH} is the Schwarzschild radius of the SMBH.

This is clearly an oversimplified scenario of accretion of galaxy mass onto a SMBH which has, in reality, a much more complex physics involved. At least,

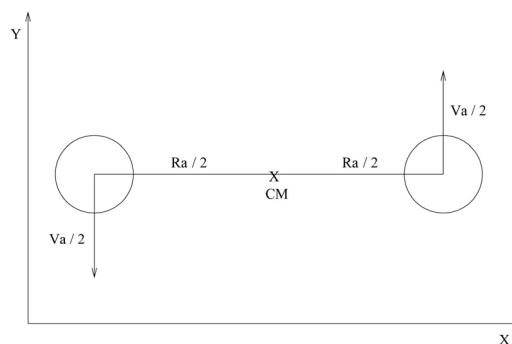


Figure 1. Schematic plot showing the initial positions and velocities of the primary and secondary galaxies. The quantities R_a and V_a are given in **Table 3** and **Table 4**. CM denotes the center of the mass of the binary.

this study, we can know approximately the evolution of the SMBH mass and its dynamical evolution in binary galaxies during a long-time evolution.

In order to determine the number of bulge/halo/disk particles accreted onto the SMBH as a function of time, we have saved a snapshot at each time step of 4.9 time units until the Hubble time $t_H = 490$ of both galaxies, primary and secondary. Thus, at the end of each experiment we have 100 saved snapshot files. Each snapshot file generated by the modified GADGET code has an identification number, position, velocity and mass of each particle. In this way we can identify the bulge/halo/disk galaxy structure that each particle belongs. When a given particle is merged with the SMBH, using the condition (2), we sum the mass of this particle with the previous mass of the SMBH and set zero mass to this particle. Besides, we recalculate the new position and velocity of the SMBH after the inelastic collision and then we let evolve the system again. At the end of each experiment we count how many bulge/halo/disk particles with zero mass that certainly have merged with the SMBH. Thus, we can obtain the time evolution of the bulge/halo/disk accreted onto the SMBH.

3. Initial Conditions of the Simulations

We have utilized the self-consistent disc-bulge-halo galaxy model by Kuijken & Dubinski [32] in the simulations, the same as in our previous paper [29] (see [Table 1](#) and [Table 2](#)). We have also introduced a SMBH seed at rest and at the center of the mass of the galaxy, in order to study its mass and dynamical evolution.

Our simulations have been utilized fewer particles than other works on gas-free galaxies but without an initial SMBH seed. In order to try to answer the questions proposed here, we have run small simulations using the available computer clusters, to have, at least, an initial mass and dynamical study of the SMBH seed.

Table 1. Disc galaxy model properties.

Galaxy	M_d	N_d	R_d	Z_d	R_t	M_b	N_b	M_h	N_h
G_1	0.871	40,000	1.000	0.100	5.000	0.425	19,538	4.916	225,880

M_d is the disc mass, N_d the number of particles of the disc, R_d the disc scale radius, Z_d the disc scale height, R_t the disc truncation radius, M_b the bulge mass, N_b the number of particles in the bulge, M_h the halo mass, N_h the number of halo particles.

Table 2. Continuation of [Table 1](#).

Galaxy	m	ϵ	M_{BH}	R_{bh}
G_1	2.1764×10^{-5}	8.0000×10^{-4}	2.1764×10^{-4}	2.3597×10^{-10}

m the mass of each particle, and ϵ is the softening of each particle. M_{bh} the SMBH mass, R_{bh} the SMBH radius.

4. The Results of the Simulations

We have run several simulations, without the secondary galaxy to check the initial structure of the galaxy model with the initial SMBH seed at rest at its center (see **Figures 2-6**). For the simulations with the primary and secondary galaxies we have used two clusters: SGI ICE-X and BULL-X BLADE B500, The maximum number of CPU processors have used for both clusters were 32. Each simulation took about 45 days (BULL-X BLADE B500) and 31 days (SGI ICE-X) of CPU time on average.

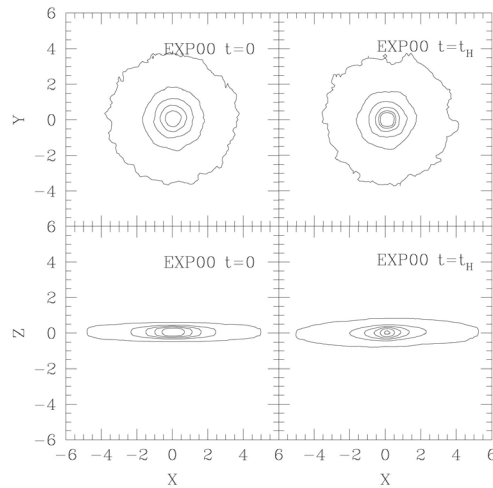


Figure 2. Contour plot of the primary galaxy G_1 at the times $t=0$ and $t=t_H$). The smoothing was made by averaging the 25 first and second neighbors of each pixel. The density levels in the planes XY and XZ at $t=0$ are used in contour plots, in the planes XY and XZ at $t=t_H$.

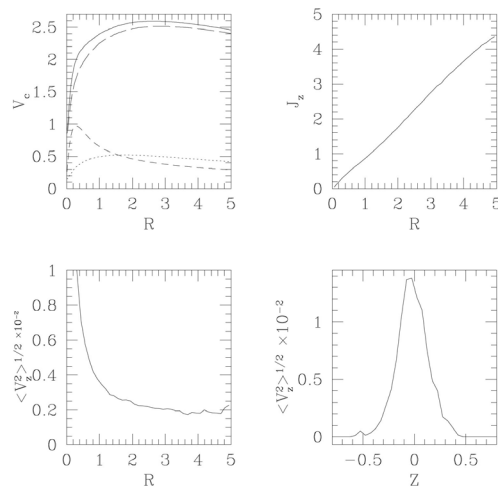


Figure 3. Rotation curve of the galaxy G_1 of the disc V_c , the angular momentum per unit of mass J_z and the velocity dispersion in the z direction $\langle V_z^2 \rangle^{1/2}$ at the time $t=0$. Hereinafter, the coordinate R is the radius in cylindrical coordinates. The dotted line denotes the disc, the long-dashed line denotes the bulge, the short-dashed line denotes the halo, and the solid line denotes the total rotation curve.

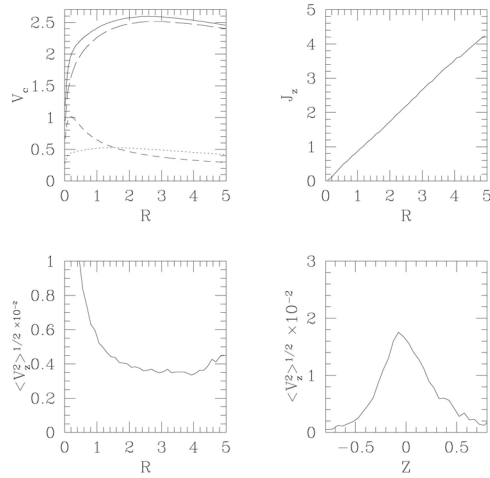


Figure 4. Rotation curve of the galaxy G_1 of the disc V_c , the angular momentum per unit of mass J_z and the velocity dispersion in the z direction $\langle V_z^2 \rangle^{1/2}$ at the time $t = t_H$. The dotted line denotes the disc, the long-dashed line denotes the bulge, the short-dashed line denotes the halo, and the solid line denotes the total rotation curve.

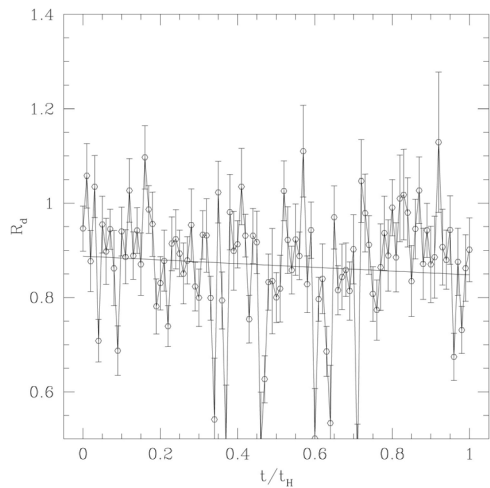


Figure 5. The evolution in time of the scale radius R_d . The projected particle number density on the XY plane was fitted using the sech disc approximation for each instant of time. This approximation was also used in our previous work [29]. The linear fitting parameters are $R_d = (0.8878 \pm 0.1993 \times 10^{-1})[t/t_H] + (0.8878 \pm 0.1993 \times 10^{-1})$.

In **Figure 2** we show the contour plot of the primary galaxy at the beginning of the simulation ($t = 0$) and at the Hubble time of the simulation ($t = t_H$). We note that the central density in the plane XY has increased slightly after one Hubble time of simulation, since the contour levels are the same for the two moments of time.

Comparing **Figure 3** and **Figure 4**, we note from the quantity $\langle V_z^2 \rangle^{1/2}$ that the self-heating of the initial disc and the particle halo adds a significant source of heating in the disc. The softening can also cause the disc to heat up. Moreover, the total rotation curves V_c and the angular momentum in the Z direction have

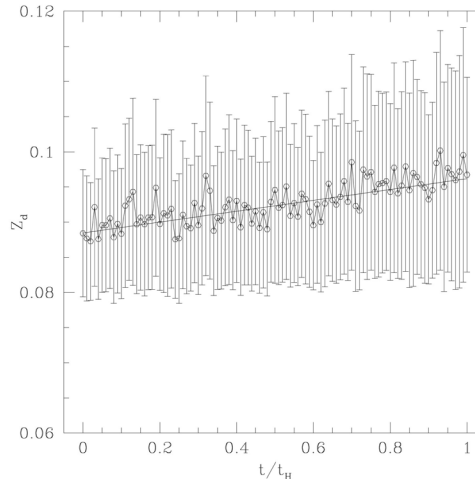


Figure 6. The evolution in time of the scale height Z_d . The projected particle number density on the XZ plane was fitted using the sech disc approximation for each instant of time, as used in our previous work [29]. The linear fitting parameters are $Z_d = (0.8848 \times 10^{-1} \pm 0.3456 \times 10^{-3})[t/t_H] + (0.7696 \times 10^{-2} \pm 0.6771 \times 10^{-3})$.

not changed at the time $t = t_H$ of the simulation. The maximum of the rotation curve $V_c^{\max} = 2.5$ occurs when $R_{\max} = 2$.

In **Figure 5** and **Figure 6** we present the temporal evolution of the scale radius R_d and the scale height Z_d . Because of the heating of the disc, the first quantity diminishes with the time while the second increases with the time. The linear fitting parameters of these two quantities are presented in the captions of these figures. In the XZ plane, the scale height has increased 8% because of the two-body relaxation heating (**Figure 6**).

Comparing all the results presented in **Figures 2-6** with our previous work [(Chan Junqueira 2014)] at $t = t_H$ for the same quantities we can show that they are very similar to ours here, except the rotation curve V_c (**Figure 4**) and the scale height Z_d (**Figure 6**). In the previous paper, we have obtained that the maximum of the rotation curve $V_c^{\max} = 1.2$ occurs at $R_{\max} = 0.2$ and the scale height Z_d increased only 0.2%. The differences are caused mainly because of the initial SMBH seed.

All the initial conditions of the numerical experiments are presented in **Table 3** and **Table 4**. The orbits of the initial galaxies are eccentric ($e = 0.1, 0.4$ or 0.7) and the orientations of the discs are coplanar ($\Theta = 0$) or polar ($\Theta = 90$) to each other. The simulations always have begun with the primary and secondary galaxies at the apocentric positions.

We will show only the evolution time of the SMBH of the experiments where the two discs merge or graze each other, where the tidal effects are more prominent during the evolution of the simulation (see **Table 5** and **Table 6**). The experiments are EXP02, EXP06, EXP20 and EXP24.

Comparing the contour plots of the discs at $t = t_H$ shown in **Figure 7** for the experiments EXP02 and EXP20 we can note that the merger of the primary and

Table 3. Primary and secondary galaxy initial conditions.

EXP	Θ	R_p	e	R_a	V_a	M_{bh}
00						2.1764×10^{-4}
01	0	12	0.1	14.67	0.8732	2.1764×10^{-4}
02	0	12	0.4	28.00	0.5160	2.1764×10^{-4}
03	0	12	0.7	68.00	0.2341	2.1764×10^{-4}
04	0	15	0.1	18.33	0.7810	2.1764×10^{-4}
05	0	15	0.4	35.00	0.4615	2.1764×10^{-4}
06	0	15	0.7	85.00	0.2094	2.1764×10^{-4}
07	0	20	0.1	24.44	0.6763	2.1764×10^{-4}
08	0	20	0.4	46.67	0.3997	2.1764×10^{-4}
09	0	20	0.7	113.33	0.1814	2.1764×10^{-4}
10	0	23	0.1	28.11	0.6307	2.1764×10^{-4}
11	0	23	0.4	53.67	0.3727	2.1764×10^{-4}
12	0	23	0.7	130.33	0.1691	2.1764×10^{-4}
13	0	25	0.1	30.56	0.6049	2.1764×10^{-4}
14	0	25	0.4	58.33	0.3575	2.1764×10^{-4}
15	0	25	0.7	141.67	0.1622	2.1764×10^{-4}
16	0	30	0.1	36.67	0.5522	2.1764×10^{-4}
17	0	30	0.4	70.00	0.3263	2.1764×10^{-4}
18	0	30	0.7	170.00	0.1481	2.1764×10^{-4}

Θ the angle between the two planes of the discs in units of degree, R_p the pericentric distance, M_1 the primary galaxy mass, e the eccentricity, R_a the apocentric distance, V_a the velocity at the apocentric distance, M_1 the primary galaxy mass, and $M_2 = M_1 = 0.621$ is the secondary mass galaxy. In these experiments the orbits of the particles of both galaxies, primary and secondary galaxy, have clockwise rotations.

Table 4. Continuation of **Table 3.**

EXP	Θ	R_p	e	R_a	V_a	M_{bh}
19	90	12	0.1	14.67	0.8732	2.1764×10^{-4}
20	90	12	0.4	28.00	0.5160	2.1764×10^{-4}
21	90	12	0.7	68.00	0.2341	2.1764×10^{-4}
22	90	15	0.1	18.33	0.7810	2.1764×10^{-4}
23	90	15	0.4	35.00	0.4615	2.1764×10^{-4}
24	90	15	0.7	85.00	0.2094	2.1764×10^{-4}
25	90	20	0.1	24.44	0.6763	2.1764×10^{-4}
26	90	20	0.4	46.67	0.3997	2.1764×10^{-4}
27	90	20	0.7	113.33	0.1814	2.1764×10^{-4}
28	90	23	0.1	28.11	0.6307	2.1764×10^{-4}

Continued

29	90	23	0.4	53.67	0.3727	2.1764×10^{-4}
30	90	23	0.7	130.33	0.1691	2.1764×10^{-4}
31	90	25	0.1	30.56	0.6049	2.1764×10^{-4}
32	90	25	0.4	58.33	0.3575	2.1764×10^{-4}
33	90	25	0.7	141.67	0.1622	2.1764×10^{-4}
34	90	30	0.1	36.67	0.5522	2.1764×10^{-4}
35	90	30	0.4	70.00	0.3263	2.1764×10^{-4}
36	90	30	0.7	170.00	0.1481	2.1764×10^{-4}

Θ the angle between the two planes of the discs in units of degree, R_p the pericentric distance, M_1 the primary galaxy mass, e the eccentricity, R_a the apocentric distance, V_a the velocity at the apocentric distance, M_1 the primary galaxy mass, and $M_2 = M_1 = 0.621$ is the secondary mass galaxy. In these experiments, the orbits of the particles of both galaxies, primary and secondary galaxy, have clockwise rotations.

Table 5. Characteristics of galaxy orbits and SMBH mass at t_H .

EXP	Disc Interaction	Primary SMBH	Secondary SMBH
01	Merge	58.0533	16.7611*
02	Merge	60.1646	21.8667*
03	Merge	63.4899	23.3100*
04	Merge	52.2800	33.8553
05	Merge	58.4970	14.4299*
06	Graze	60.1646	31.9683
07	Merge	59.1651	29.4152
08	Merge	67.0445	31.9678
09	Distant	57.4974	17.3160
10	Merge	59.4966	30.7468
11	Distant	58.9406	23.8649
12	Distant	62.9391	16.4281
13	Merge	60.7155	31.3022
14	Distant	61.9394	22.9770
15	Distant	61.3836	18.6481
16	Distant	58.7214	27.3059
17	Distant	64.2702	21.3118
18	Distant	60.2718	15.4290

Initial mass of SMBH of the primary and secondary galaxy is 1.1099, Primary SMBH and Secondary SMBH in units of $10^7 M_\odot$, *Graze* means that the two discs touch each other for a while and then separate. *Merge* means that the two discs fuse. *Distant* means the two discs interact apart each other. The symbol (*) after the mass of the SMBH of some merging experiments means that the SMBH has been ejected out of the binary system during the evolution of the merged binary.

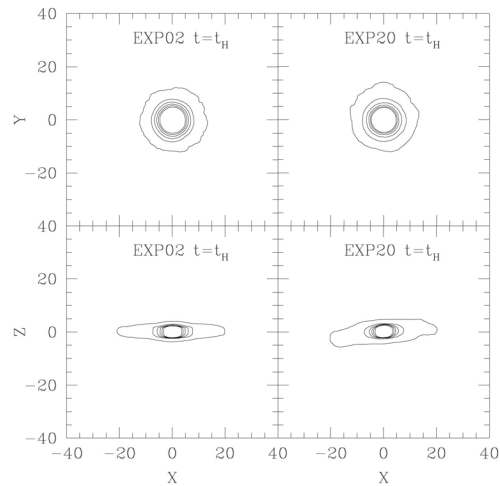


Figure 7. Contour plots of the final merged discs at $t = t_H$ of the experiments EXP02 and EXP20.

Table 6. Continuation of Table 5.

EXP	Disc Interaction	Primary SMBH	Secondary SMBH
19	Merge	53.6111	26.8622
20	Merge	52.1679	6.5489*
21	Merge	62.0517	16.5387*
22	Merge	53.3919	27.3059
23	Merge	54.1670	13.8750
24	Graze	57.9411	21.5337
25	Merge	54.8352	14.2080
26	Merge	62.0517	21.8667
27	Distant	58.1654	21.2012
28	Merge	58.8284	23.4212
29	Distant	60.4962	24.3091
30	Distant	61.3836	18.8700
31	Merge	61.8273	21.3118
32	Distant	62.3832	21.3118
33	Distant	61.7151	21.7560
34	Distant	61.6029	24.8640
35	Distant	59.3843	21.9779
36	Distant	61.0521	21.2007

Initial mass of SMBH of the primary and secondary galaxy is 1.1099, Primary SMBH and Secondary SMBH in units of $10^7 M_\odot$, *Graze* means that the two discs touch each other for a while and then separate. *Merge* means that the two discs fuse. *Distant* means the two discs interact apart each other. The symbol (*) after the mass of the SMBH of some merging experiments means that the SMBH has been ejected out of the binary system during the evolution of the merged binary.

secondary discs can result in a final normal disc (EXP02) or a final warped disc (EXP20). After the fusion of discs, the final one is thicker and larger than the initial discs.

In **Figures 8(a)-11(a)** we show the time evolution of the SMBH mass of the primary and secondary galaxy of the experiments EXP02, EXP06, EXP20 and EXP24. We also present the time evolution of the SMBH mass of the isolated galaxy in **Figures 8(a)-11(a)**, in order to compare its SMBH mass growth to the SMBH mass growth of the primary and secondary galaxy during the evolution. In the same plots, we show the temporal evolution of the distance of

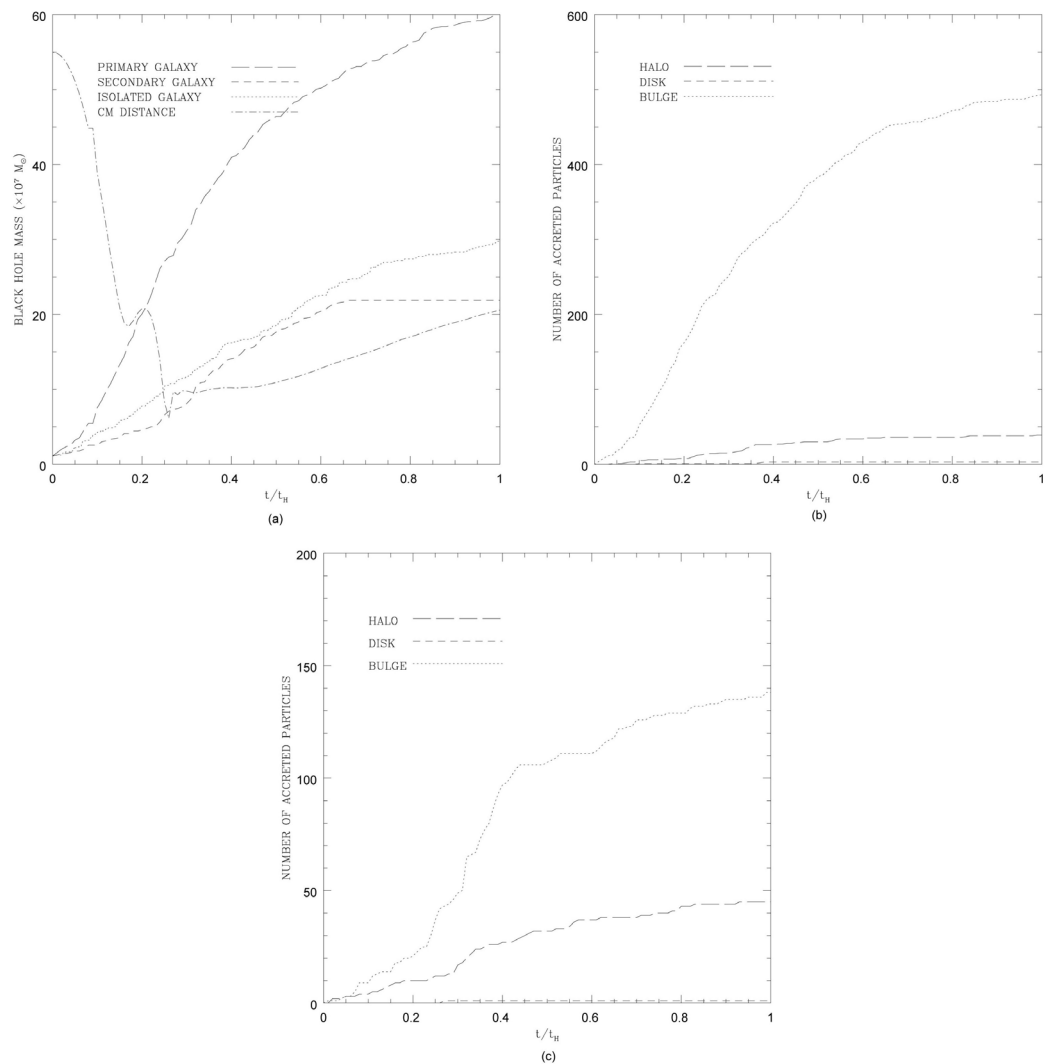


Figure 8. (a) Temporal evolution of the SMBH seed mass of the primary (long-dashed line) and secondary galaxy (short-dashed line) of the experiment EXP02. We also present the time evolution of the SMBH seed mass of the isolated galaxy. In the same plot we show the temporal evolution of the distance of the center of mass of the two galaxies (dot-dashed line). There is an arbitrary scale factor only to adjust the distance within the plot scale. (b) and (c) Time evolution of the number of accreted particles of the primary and secondary galaxy onto the SMBH. The long-dashed lines represent the halo particles. The dotted lines represent the bulge particles. The short-dashed lines represent the disk particles. (a) EXP02; (b) EXP02 (primary galaxy); (c) EXP02 (secondary galaxy).

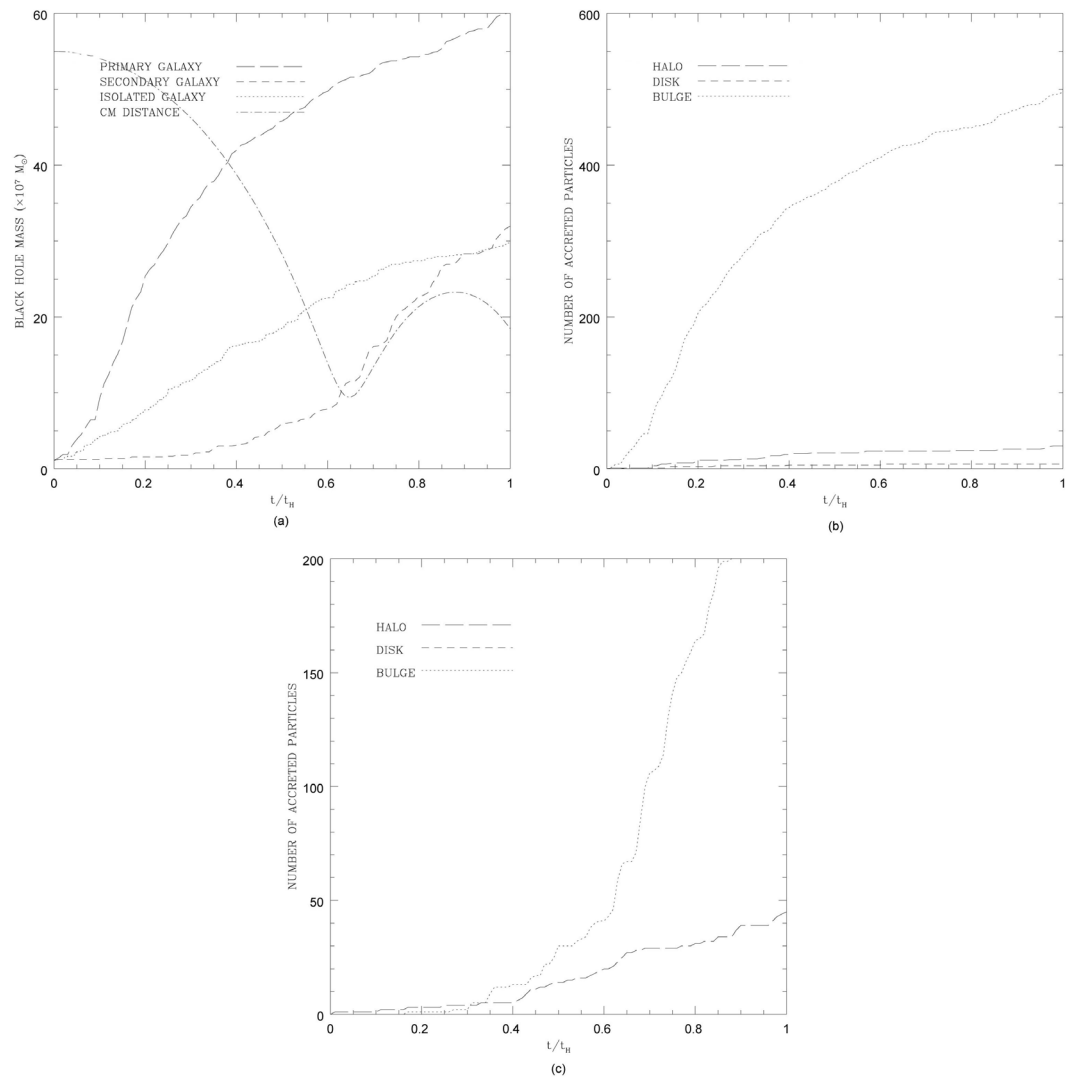


Figure 9. (a) Temporal evolution of the SMBH seed mass of the primary (long-dashed line) and secondary galaxy (short-dashed line) of the experiment EXP06. We also present the time evolution of the SMBH seed mass of the isolated galaxy. In the same plot, we show the temporal evolution of the distance of the center of mass of the two galaxies (dot-dashed line). There is an arbitrary scale factor only to adjust the distance within the plot scale. (b) and (c) Time evolution of the number of accreted particles of the primary and secondary galaxy onto the SMBH. The long-dashed lines represent the halo particles. The dotted lines represent the bulge particles. The short-dashed lines represent the disk particles. (a) EXP06; (b) EXP06 (primary galaxy); (c) EXP06 (secondary galaxy).

the center of mass between the two galaxies. There is an arbitrary scale factor only to adjust the distance within the plot scale of each figure. The purpose of these plots is to know if the distance approach of the primary and secondary galaxies to each other increases the mass growth of the SMBHs.

Figures 8(b)-11(b) and **Figures 8(c)-11(c)** show the time evolution of the number of accreted particles of the primary and secondary galaxy onto the SMBHs, respectively. These plots show how many halo, bulge and disc particles that contribute to the growth of SMBH mass.

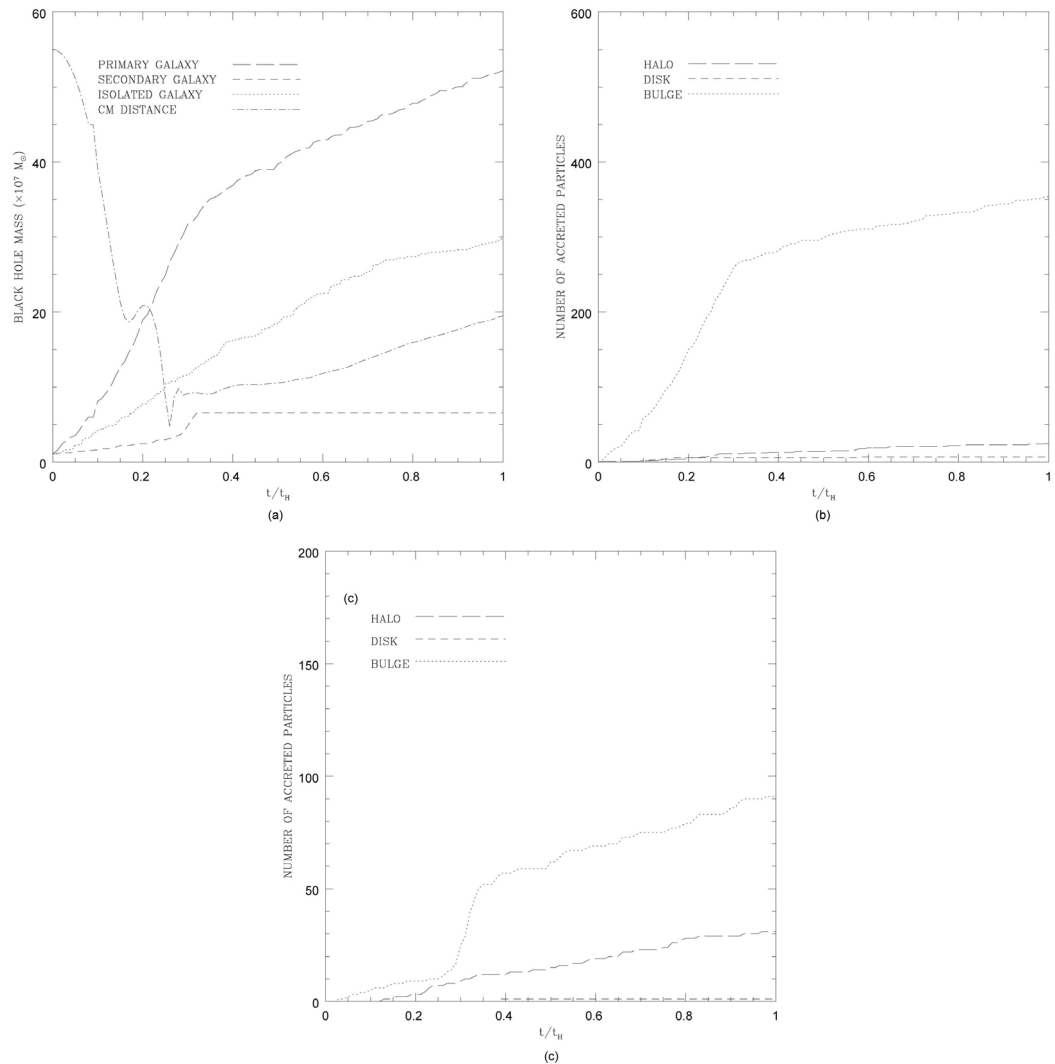


Figure 10. (a) Temporal evolution of the SMBH seed mass of the primary (long-dashed line) and secondary galaxy (short-dashed line) of the experiment EXP20. We also present the time evolution of the SMBH seed mass of the isolated galaxy. In the same plot we show the temporal evolution of the distance of the center of mass of the two galaxies (dot-dashed line). There is an arbitrary scale factor only to adjust the distance within the plot scale. (b) and (c) Time evolution of the number of accreted particles of the primary and secondary galaxy onto the SMBH. The long-dashed lines represent the halo particles. The dotted lines represent the bulge particles. The short-dashed lines represent the disk particles. (a) EXP20; (b) EXP20 (primary galaxy); (c) EXP20 (secondary galaxy).

Comparing **Figures 8(a)-11(a)** we can notice the tidal effects in the SMBH mass of the secondary galaxy are more important (see the distance of the center of mass between the two galaxies in the plot). The approach of the galaxies to each other seems not to affect too much the primary galaxy (see **Table 5** and **Table 6**).

Comparing **Figures 8(b)-11(b)** and **Figures 8(c)-11(c)**, respectively, we can note that most of the accreted particles onto the SMBH have come from the bulges and from the halos. Only a small number of the accreted particles onto the SMBH has come from the discs.

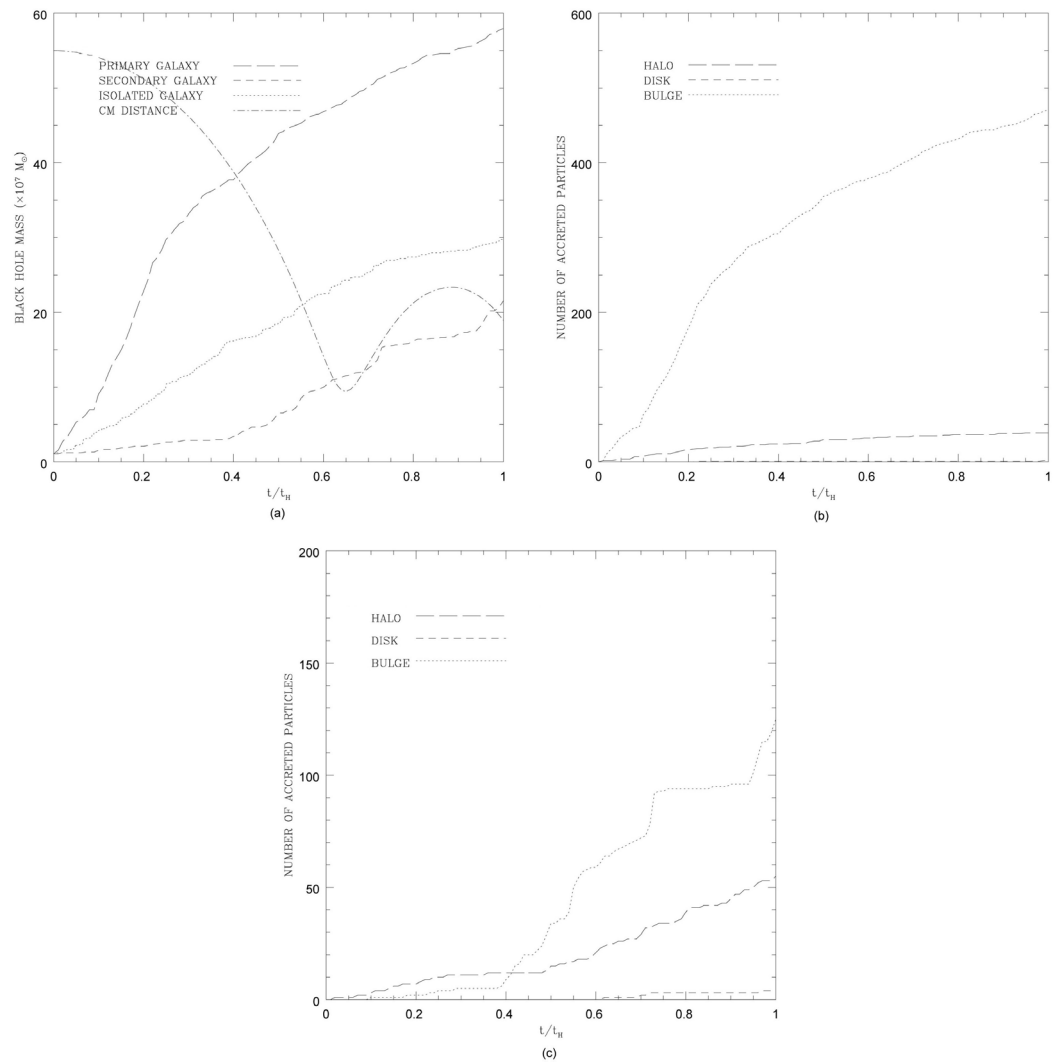


Figure 11. (a) Temporal evolution of the SMBH seed mass of the primary (long-dashed line) and secondary galaxy (short-dashed line) of the experiment EXP24. We also present the time evolution of the SMBH seed mass of the isolated galaxy. In the same plot we show the temporal evolution of the distance of the center of mass of the two galaxies (dot-dashed line). There is an arbitrary scale factor only to adjust the distance within the plot scale. (b) and (c) Time evolution of the number of accreted particles of the primary and secondary galaxy onto the SMBH. The long-dashed lines represent the halo particles. The dotted lines represent the bulge particles. The short-dashed lines represent the disk particles. (a) EXP24; (b) EXP24 (primary galaxy); (c) EXP24 (secondary galaxy).

In some cases of final merging stage of the two galaxies, the final SMBH of the secondary galaxy is ejected out of the galaxy (see [Table 5](#) and [Table 6](#)).

From [Table 5](#) and [Table 6](#) we can see comparing the final SMBH mass of all the experiments that the mass of the SMBH of the primary galaxy have increased by a factor ranging from 52 to 64 times the initial seed mass, depending on the experiment. However, the mass of the SMBH of the secondary galaxy has increased by a factor ranging from 6 to 33 times in comparison to the initial seed mass, depending on the experiment. Thus, we can conclude that the tidal effects are very important, modifying the evolution of the SMBH in the primary and

secondary galaxy differently.

5. Conclusions

We have shown the results of N-body simulations of the interactions of two gas-free disc galaxies with the same mass. Both disc galaxies have halos of dark matter, central bulges and initial SMBH seeds at their centers.

We have found that the merger of the primary and secondary discs can result in a final normal disc or a final warped disc. After the fusion of discs, the final one is thicker and larger than the initial disc.

The tidal effects are very important, modifying the evolution of the SMBH in the primary and secondary galaxy differently. The mass of the SMBH of the primary galaxy has increased by a factor ranging from 52 to 64 times the initial seed mass, depending on the experiment. However, the mass of the SMBH of the secondary galaxy has increased by a factor ranging from 6 to 33 times the initial SMBH seed mass, depending also on the experiment.

Most of the accreted particles have come from the bulges and from the halos, depleting their particles. This could explain why the observations show that the SMBH with masses of approximately $10^6 M_{\odot}$ is found in many bulgeless galaxies [1]. However, only a small number of the accreted particles has come from the disc.

In some cases of final merging stage of the two galaxies, the final SMBH of the secondary galaxy was ejected out of the galaxy.

Acknowledgements

The author acknowledges the financial support from Conselho Nacional de Desenvolvimento Científico e Tecnológico in Brazil.

The author also thanks the generous amount of CPU time given by CENAPAD/UFC (Centro Nacional de Processamento de Alto Desempenho da UFC) and NACAD/COPPE-UFRJ (Núcleo de Avançado de Computação de Alto Desempenho da COPPE/UFRJ) in Brazil. In addition, this research has been supported by SINAPAD/Brazil.

Conflicts of Interest

The author declares no conflicts of interest regarding the publication of this paper.

References

- [1] Kormendy, J. and Ho, L.C. (2013) Coevolution (Or Not) of Supermassive Black Holes and Host Galaxies. *Annual Review of Astronomy and Astrophysics*, **51**, 511. <https://doi.org/10.1146/annurev-astro-082708-101811>
- [2] Moran, E.C., Shahinyan, K., Sugarman, H.R., Velez, D.O. and Eracleous, M. (2014) Black Holes at the Centers of Nearby Dwarf Galaxies. *The Astronomical Journal*, **148**, 136. <https://doi.org/10.1088/0004-6256/148/6/136>
- [3] Tremmel, M., Governato, F., Volonteri, M., Quinn, T.R. and Pontzen, A. (2018)

- Dancing to CHANGA: A Self-Consistent Prediction for Close SMBH Pair Formation Time-Scales Following Galaxy Mergers. *Monthly Notices of the Royal Astronomical Society*, **475**, 4967-4977. <https://doi.org/10.1093/mnras/sty139>
- [4] Sanchez, N.N., Bellovary, J.M., Holley-Bockelmann, K., Tremmel, M., Brooks, A., Governato, F., Quinn, T., Volonteri, M. and Wadsley, J. (2018) Preferential Accretion in the Supermassive Black Holes of Milky Way-size Galaxies Due to Direct Feeding by Satellites. *The Astronomical Journal*, **860**, 20. <https://doi.org/10.3847/1538-4357/aac015>
- [5] Curd, B. and Narayan, R. (2019) GRRMHD Simulations of Tidal Disruption Event Accretion Discs around Supermassive Black Holes: Jet Formation, Spectra, and Detectability. *Monthly Notices of the Royal Astronomical Society*, **483**, 565-596. <https://doi.org/10.1093/mnras/sty3134>
- [6] Springel, V., Di Matteo, T. and Hernquist, L. (2005) Modelling Feedback from Stars and Black Holes in Galaxy Mergers. *Monthly Notices of the Royal Astronomical Society*, **361**, 776-794. <https://doi.org/10.1111/j.1365-2966.2005.09238.x>
- [7] Di Matteo, T., Colberg, J., Springel, V., Hernquist, L. and Sijacki, D. (2008) Direct Cosmological Simulations of the Growth of Black Holes and Galaxies. *The Astrophysical Journal*, **676**, 33-53. <https://doi.org/10.1086/524921>
- [8] Khan, F.M., Capelo, P.R., Mayer, L. and Berczik, P. (2018) Dynamical Evolution and Merger Timescales of LISA Massive Black Hole Binaries in Disk Galaxy Mergers. *The Astrophysical Journal*, **868**, 97. <https://doi.org/10.3847/1538-4357/aae77b>
- [9] Gabor, J.M., Capelo, P.R., Volonteri, M., Bournaud, F., Bellovary, J., Governato, F. and Quinn, T. (2016) Comparison of Black Hole Growth in Galaxy Mergers with Gasoline and Ramses. *Astronomy & Astrophysics*, **592**, A62. <https://doi.org/10.1051/0004-6361/201527143>
- [10] Callegari, S., Mayer, L., Kazantzidis, S., Colpi, M., Governato, F., Quinn, T. and Wadsley, J. (2009) Pairing of Supermassive Black Holes in Unequal-Mass Galaxy Mergers. *The Astrophysical Journal*, **696**, L89. <https://doi.org/10.1088/0004-637X/696/1/L89>
- [11] Hopkins, P.F., Hernquist, L., Cox, T.J., Di Matteo, T., Martini, P., Robertson, B. and Springel, V. (2005) Black Holes in Galaxy Mergers: Evolution of Quasars. *The Astrophysical Journal*, **630**, 705-715. <https://doi.org/10.1086/432438>
- [12] Hopkins, P.F., Somerville, R.S., Hernquist, L., Cox, T.J., Robertson, B. and Li, Y. (2006) The Relation between Quasar and Merging Galaxy Luminosity Functions and the Merger-Driven Star Formation History of the Universe. *The Astrophysical Journal*, **652**, 864-888. <https://doi.org/10.1086/508503>
- [13] Mayer, L., Kazantzidis, S., Madau, P., Colpi, M., Quinn, T. and Wadsley, J. (2007) Rapid Formation of Supermassive Black Hole Binaries in Galaxy Mergers with Gas. *Science*, **316**, 1874-1877. <https://doi.org/10.1126/science.1141858>
- [14] Chapon, D., Mayer, L. and Teyssier, R. (2013) Hydrodynamics of Galaxy Mergers with Supermassive Black Holes: Is There a Last Parsec Problem? *Monthly Notices of the Royal Astronomical Society*, **429**, 3114-3122. <https://doi.org/10.1093/mnras/sts568>
- [15] Li, S., Liu, F.K., Berczik, P. and Spurzen, R. (2017) Boosted Tidal Disruption by Massive Black Hole Binaries During Galaxy Mergers from the View of N-Body Simulation. *The Astrophysical Journal*, **834**, 195. <https://doi.org/10.3847/1538-4357/834/2/195>
- [16] Governato, F., Colpi, M. and Maraschi, L. (1994) The Fate of Central Black Holes in Merging Galaxies. *Monthly Notices of the Royal Astronomical Society*, **271**,

- 317-322. <https://doi.org/10.1093/mnras/271.2.317>
- [17] Ebisuzaki, T., Makino, J. and Okumura, S.K. (1991) Merging of Two Galaxies with Central Black Holes. *Nature*, **354**, 212-214. <https://doi.org/10.1038/354212a0>
- [18] Makino, J. Fukushige, T., Okumura, S.K. and Ebisuzaki, T. (1993) The Evolution of Massive Black-Hole Binaries in Merging Galaxies. I. Evolution of a Binary in a Spherical Galaxy. *Publications of the Astronomical Society of Japan*, **45**, 303-310.
- [19] Makino, J. and Ebisuzaki, T. (1996) Merging of Galaxies with Central Black Holes. I. Hierarchical Mergings of Equal-Mass Galaxies. *The Astrophysical Journal*, **465**, 527-533. <https://doi.org/10.1086/177439>
- [20] Makino, J. (1997) Merging of Galaxies with Central Black Holes. II. Evolution of the Black Hole Binary and the Structure of the Core. *The Astrophysical Journal*, **478**, 58-65. <https://doi.org/10.1086/303773>
- [21] Khan, F.M., Berentzen, I., Berczik, P., Just, A., Mayer, L., Nitadori, K. and Callegari, S. (2012) Formation and Hardening of Supermassive Black Hole Binaries in Minor Mergers of Disk Galaxies. *The Astrophysical Journal*, **756**, 30. <https://doi.org/10.1088/0004-637X/756/1/30>
- [22] Rantala, A., Johansson, P.H., Naab, T., Thomas, J. and Frigo, M. (2018) The Formation of Extremely Diffuse Galaxy Cores by Merging Supermassive Black Holes. *The Astrophysical Journal*, **864**, 113. <https://doi.org/10.3847/1538-4357/aada47>
- [23] Oh, S.H., Kim, W., Lee, H.M. and Kim, J. (2008) Physical Properties of Tidal Features in Interacting Disk Galaxies. *The Astrophysical Journal*, **683**, 94. <https://doi.org/10.1086/588184>
- [24] Dobbs, C.L., Theis, C., Pringle, J.E. and Bate, M.R. (2010) Simulations of the Grand Design Galaxy M51: A Case Study for Analysing Tidally Induced Spiral Structure. *Monthly Notices of the Royal Astronomical Society*, **403**, 625-645. <https://doi.org/10.1111/j.1365-2966.2009.16161.x>
- [25] Lotz, J.M., Jonsson, P., Cox, T.J. and Primack, J.R. (2010) The Effect of Mass Ratio on the Morphology and Time-Scales of Disc Galaxy Mergers. *Monthly Notices of the Royal Astronomical Society*, **404**, 575-589. <https://doi.org/10.1111/j.1365-2966.2010.16268.x>
- [26] Struck, C., Dobbs, C.L. and Hwang, J. (2011) Slowly Breaking Waves: The Longevity of Tidally Induced Spiral Structure. *Monthly Notices of the Royal Astronomical Society*, **414**, 2498-2510. <https://doi.org/10.1111/j.1365-2966.2011.18568.x>
- [27] Bois, M., Emsellem, E., Bournaud, F., Alatalo, K., Blitz, L., Bureau, M., Cappellari, M., Davies, R.L., Davis, T.A., de Zeeuw, P.T., Duc, P., Khochfar, S., Krajnovi, D., Kuntschner, H., Lablanche, P., McDermid, R.M., Morganti, R., Naab, T., Oosterloo, T., Sarzi, M., Scott, N., Serra, P., Weijmans, A. and Young, L.M. (2011) The ATLAS3D Project VI. Simulations of Binary Galaxy Mergers and the Link with Fast Rotators, Slow Rotators and Kinematically Distinct Cores. *Monthly Notices of the Royal Astronomical Society*, **416**, 1654-1679. <https://doi.org/10.1111/j.1365-2966.2011.19113.x>
- [28] Chan, R. and Junqueira, S. (2003) Morphological and Kinematic Properties of Disk Galaxies Perturbed by a Satellite. *The Astrophysical Journal*, **586**, 780-793. <https://doi.org/10.1086/367765>
- [29] Chan, R. and Junqueira, S. (2014) Long-Time Evolution of Gas-Free Disk Galaxies in Binary Systems. *Astronomy & Astrophysics*, **567**, A17. <https://doi.org/10.1051/0004-6361/201423656>
- [30] Chan, R. and Junqueira, S. (2001) The Orbital Evolution of Binary Galaxies. *Astronomy & Astrophysics*, **366**, A418. <https://doi.org/10.1051/0004-6361:20000256>

- [31] Springel, V., Yoshida, N. and White, S.D.M. (2001) GADGET: A Code for Collisionless and Gasdynamical Cosmological Simulations. *New Astronomy*, **6**, 79-117.
[https://doi.org/10.1016/S1384-1076\(01\)00042-2](https://doi.org/10.1016/S1384-1076(01)00042-2)
- [32] Kuijken, K. and Dubinski, J. (1995) Nearly Self-Consistent Disc/Bulge/Halo Models for Galaxies. *Monthly Notices of the Royal Astronomical Society*, **277**, 1341-1353.
<https://doi.org/10.1093/mnras/277.4.1341>